Neuro-Oncology Advance Access published December 21, 2014

Neuro-Oncology

Neuro-Oncology 2014; **0**, 1–11, doi:10.1093/neuonc/nou329

Akt- or MEK-mediated mTOR inhibition suppresses *Nf1* optic glioma growth

Aparna Kaul, Joseph A. Toonen, Patrick J. Cimino, Scott M. Gianino, and David H. Gutmann

Department of Neurology, Washington University School of Medicine, St. Louis, Missouri (A.K., J.A.T., S.M.G., D.H.G.); Department of Pathology, Washington University School of Medicine, St. Louis, Missouri (P.J.C.)

Corresponding Author: David H. Gutmann, MD, PhD, Department of Neurology, Washington University, Box 8111, 660 S. Euclid Avenue, St. Louis, MO 63110 (gutmannd@neuro.wustl.edu).

Background. Children with neurofibromatosis type 1 (NF1) develop optic pathway gliomas, which result from impaired *NF1* protein regulation of Ras activity. One obstacle to the implementation of biologically targeted therapies is an incomplete understanding of the individual contributions of the downstream Ras effectors (mitogen-activated protein kinase kinase [MEK], Akt) to optic glioma maintenance. This study was designed to address the importance of MEK and Akt signaling to *Nf1* optic glioma growth.

Methods. Primary neonatal mouse astrocyte cultures were employed to determine the consequence of phosphatidylinositol-3 kinase (PI3K)/Akt and MEK inhibition on *Nf1*-deficient astrocyte growth. *Nf1* optic glioma–bearing mice were used to assess the effect of Akt and MEK inhibition on tumor volume, proliferation, and retinal ganglion cell dysfunction.

Results. Both MEK and Akt were hyperactivated in *Nf1*-deficient astrocytes in vitro and in *Nf1* murine optic gliomas in vivo. Pharmacologic PI3K or Akt inhibition reduced *Nf1*-deficient astrocyte proliferation to wild-type levels, while PI3K inhibition decreased *Nf1* optic glioma volume and proliferation. Akt inhibition of *Nf1*-deficient astrocyte and optic glioma growth reflected Akt-dependent activation of mammalian target of rapamycin (mTOR). Sustained MEK pharmacologic blockade also attenuated *Nf1*-deficient astrocytes as well as *Nf1* optic glioma volume and proliferation. Importantly, these MEK inhibitory effects resulted from p90RSK-mediated, Akt-independent mTOR activation. Finally, both PI3K and MEK inhibition reduced optic glioma–associated retinal ganglion cell loss and nerve fiber layer thinning.

Conclusion. These findings establish that the convergence of 2 distinct Ras effector pathways on mTOR signaling maintains *Nf1* mouse optic glioma growth, supporting the evaluation of pharmacologic inhibitors that target mTOR function in future human NF1–optic pathway glioma clinical trials.

Keywords: MEK, mTOR, neurofibromin, optic glioma, PI3K/Akt.

Neurofibromatosis type 1 (NF1) is one of the most common inherited cancer syndromes in which affected individuals develop brain tumors.[1] As such, children with NF1 are at risk for the formation of low-grade glial neoplasms involving the optic pathway (optic nerve, chiasm, and postchiasmal tracts; optic pathway glioma [OPG]),[2,3] which can lead to visual impairment.[4,5] Since surgery is not an option because of permanent nerve damage, and radiation therapy is associated with an increased incidence of fatal secondary high-grade glioma,[6] the mainstay of treatment has been chemotherapy. For the past 25 years, the treatment of NF1-OPG has largely employed anti-neoplastic agents used for sporadic low-grade glioma[7,8] with varying success.

Genetically engineered mouse (GEM) models provide unprecedented opportunities to identify and critically evaluate therapies specifically targeted to NF1-OPG. To this end, *Nf1*+/− mice with neuroglial progenitor *Nf1* loss develop low-grade gliomas of the prechiasmatic optic nerves and chiasm with many similarities to their human counterparts.[9,10] As observed in human NF1-OPG, these murine tumors harbor low proliferative indices, microglia infiltration, nuclear pleomorphism, cellular atypia, and bipolar neoplastic glial cells. *Nf1* optic glioma mice have been previously employed to demonstrate that increased cell growth results from loss of *Nf1* protein (neurofibromin) regulation of Ras in neuroglial progenitors, leading to elevated Ras and Ras pathway activation.[11] The critical role of deregulated Ras signaling in *Nf1* optic glioma formation is further underscored by the finding that *Nf1*+/− mice with constitutively active *KRas* expression in neuroglial progenitors develop optic glioma.[12]

Received 14 June 2014; accepted 8 November 2014

Ras transmits its growth regulatory signal through downstream signaling intermediates, including protein kinase-B (Akt) and mitogen activated protein kinase (ERK). While previous studies from our laboratory have identified the Akt/mammalian target of rapamycin (mTOR) effector arm as a major regulator of *Nf1* optic glioma growth,[11,13] recent reports have demonstrated that ERK is the primary driver of tumor growth in other NF1-associated cancers.[14,15] These observations have prompted recent clinical trials employing inhibitors of mitogen-activated protein kinase kinase (MEK) for the treatment of plexiform neurofibromas (NCT01362803) and brain tumors (NCT01885195) in individuals with NF1.

In this report, we sought to critically establish which Ras effector pathway is responsible for maintaining *Nf1* optic glioma growth. Using a series of pharmacologic studies on *Nf1*-deficient astrocytes in vitro and *Nf1* murine optic gliomas in vivo, we demonstrate that both phosphatidylinositol-3 kinase (PI3K)/Akt and MEK/ERK signaling pathways are responsible for neurofibromin regulation of mTOR activity, such that sustained inhibition of either PI3K or MEK activity suppresses *Nf1* optic glioma proliferation and retinal ganglion cell (RGC) death in vivo. Together, these data provide further support for the use of agents that target mTOR as biologically based NF1-OPG treatments.

Materials and Methods

Human Specimens

The use of human subject materials was approved by the institutional review board of the Washington University School of Medicine. Four NF1-related pediatric intracranial pilocytic astrocytomas and 4 surgically obtained age-matched normal brain control cases were identified. Corresponding formalin-fixed paraffin-embedded blocks from the pathology archives were used for immunohistochemistry.

Mice

Nf1$^{flox/mut}$; glial fibrillary acidic protein (GFAP)–Cre (FMC) mice were generated as previously described[10] and maintained on a C57Bl/6 background. All mice were used in accordance with approved animal studies protocols at the Washington University School of Medicine.

Preclinical Therapeutic Trials

Three-month-old FMC mice from different litters were randomly assigned to control or treatment arms. For the MEK inhibition studies, mice received PD0325901 (Selleck) or hydroxypropyl methylcellulose (Sigma-Aldrich)–based vehicle by oral gavage twice a day, 6 days/week for 4 weeks. For the PI3K inhibition studies, mice received NVP-BKM120 (Novartis) or *N*-methyl-2-pyrrolidone (NMP)/PEG300 (10/90v/v)–based vehicle[16] 5 days/week for 4 weeks. Each experimental group contained 6–10 mice. *Nf1*$^{flox/flox}$ mice ($n = 6$) served as wild-type controls.

Optic Nerve Measurements

Optic nerves with an intact chiasm were microdissected and photographed and the optic nerve diameters measured at the chiasm (~150, ~300, and ~450 microns anterior to the chiasm) to generate optic nerve volumes, as previously reported.[13]

Primary Astrocyte Cultures

Wild-type and *Nf1*-deficient (*Nf1*−/−) primary astrocyte cultures were generated from the brainstems of postnatal day 1–2 mouse pups following infection with adenovirus type 5 containing β-galactosidase (Ad5-LacZ) or Cre recombinase (Ad5-Cre) (University of Iowa Gene Transfer Vector Core), respectively.[17] Retroviral transduction was used to express myristoylated Akt (myrAkt; Addgene) with empty pBABEpuro serving as control virus. Astrocyte proliferation was assessed using the BrdU Cell Proliferation ELISA kit (Roche) according to the manufacturer's instructions. Astrocytes were serum starved for 24 h followed by treatment with PD0325901 (Selleck), MK2206 (Selleck), or BKM120 (Novartis) for another 24 h in serum-free media.

Western Blotting

Mouse brains or cells were lysed in buffer containing 1% NP-40 (nonyl phenoxypolyethoxylethanol), supplemented with protease and phosphatase inhibitors. Western blotting was performed as described previously[18] using ERK, pERK$^{T202/Y204}$, Akt, pAkt^{T308} (#2965 for brain lysates and #9275 cultured astrocytes), pAkt^{S473}, S6, pS6$^{S240/244}$, pS6$^{S235/236}$, ribosomal S6 kinase (RSK), pRSK^{T573} (Cell Signaling Technology), neurofibromin (Santa Cruz Biotechnology), and α-tubulin (Sigma) antibodies.

Immunohistochemistry

Optic nerves were prepared for sectioning and immunostaining using pERK$^{T202/Y204}$, pS6$^{Ser240/244}$ (Cell Signaling Technology), and Ki67 (Abcam) antibodies as previously described.[19] Biotinylated secondary antibodies (Vector Laboratories) were used in combination with Vectastain Elite ABC development and hematoxylin counterstaining.

Retinal Analysis

Cells positive for terminal deoxynucleotidyl transferase deoxyuridine triphosphate nick end labeling (TUNEL) were expressed as a percentage of the total number of cells positive for 4′,6′-diamidino-2-phenylindole within the RGC layer,[13] while the number of Brn3a^{+} cells per 10× field were normalized to age-matched *Nf1*$^{flox/flox}$ (FF) (wild-type) mice ($n = 4$).[20] Retinal nerve fiber layer (RNFL) thickness was quantitated using the average of 15 measurements of SMI-32–stained axons 0–250 μm proximal to the optic nerve head (ImageJ software).[20]

Statistical Analysis

All in vitro experiments were performed on independent litters and repeated at least 3 times. Data were analyzed using

GraphPad Prism 5.0 software using a 2-tailed Student's *t*-test, with statistical significance set at $P < .05$.

Results

Neurofibromin Loss Results in Both Akt and ERK Activation

One of the major functions of the neurofibromin GTPase-activating protein is the negative regulation of Ras activity, leading to increased activation of Ras and its downstream effectors following *NF1* gene inactivation.[21,22] To determine which Ras effector is hyperactivated following *Nf1* inactivation in glial cells and gliomas relevant to NF1-associated optic glioma, we employed primary murine brainstem astrocytes (>97% $GFAP^+$ cells) in vitro and *Nf1* GEM optic gliomas in vivo.[10] Since optic nerve astrocyte cultures contain a mixed population of glial cells, of which only 30% are $GFAP^+$ cells that hyperproliferate following *Nf1* gene inactivation,[23] we chose brainstem astrocytes for these experiments. Moreover, the brainstem is the second most common region where gliomas arise in children with NF1.[24]

Following *Nf1* inactivation, brainstem astrocytes exhibited 2.4-fold and 2-fold increases in $ERK^{T202/Y204}$ and Akt^{T308} phosphorylation, indicative of Raf/MEK/ERK and PI3K/Akt hyperactivation, respectively (Fig. 1A). Consistent with previous reports,[11,25,26] *Nf1* loss in brainstem astrocytes also led to mTOR activation, as reflected by a 1.9-fold increase in ribosomal $S6^{S240/244}$ phosphorylation. Similarly, using *Nf1*+/− mice in which *Nf1* loss is targeted to neuroglial progenitor cells ($Nf1^{flox/mut}$; GFAP-Cre mice, FMC mice), increased pERK and pS6 staining was observed in the optic gliomas relative to wild-type mouse optic nerves (Fig. 1B). Because human optic gliomas are rarely biopsied, we used 4 NF1-associated pediatric intracranial pilocytic astrocytomas to verify these findings in human tumors. Similar to the mouse optic gliomas, we observed an increase in the intensity and frequency of pERK and pS6 positive staining (Fig. 1C). Together, these findings demonstrate that Ras activation, as a consequence of neurofibromin loss, leads to activation of both the Raf/MEK/ERK and PI3K/Akt pathways, concomitant with mTOR activation in vitro and in vivo.

Neurofibromin Regulates Astrocyte Proliferation in a PI3K/Akt-Dependent Manner

To identify the RAS effector pathway critical for neurofibromin regulation of astrocyte growth and gliomagenesis, we first focused on the PI3K/Akt pathway. We employed several complementary approaches to determine whether PI3K/Akt signaling was responsible for neurofibromin control of astrocyte proliferation. First, ectopic expression of a membrane-targeted constitutively active Akt (myrAkt) molecule[27] resulted in a 1.5-fold increase in brainstem astrocyte proliferation in vitro, concomitant with increased activation of both Akt (Thr308 and Ser473 phosphorylation) and mTOR (S6-Ser240/244 phosphorylation) relative to vector-transduced controls (Fig. 2A and Supplementary Fig. S1A). These results are in accordance with our previous observations that activation of the PI3K pathway, as a consequence of phosphatase and tensin homolog loss, results in mTOR activation and increased astrocyte proliferation.[25] Second, we used a specific inhibitor of Akt, MK2206,[28] to determine whether *Nf1* loss increased astrocyte proliferation in an Akt-dependent manner. Treatment of *Nf1*−/− astrocytes with 50 nM MK2206 inhibited Akt and S6 activation and reduced proliferation to wild-type levels (Fig. 2B and Supplementary Fig. S1B), without affecting ERK phosphorylation (Thr202/Tyr204; Supplementary Fig. S2A). Finally, treatment with the PI3K inhibitor BKM120[16] also reduced *Nf1*-deficient astrocyte proliferation (Fig. 2C) and inhibited Akt (Thr308 phosphorylation) and S6 (Ser240/244 phosphorylation) activation (Fig. 2C and Supplementary Fig. S1C) in *Nf1*-deficient astrocytes, without affecting ERK phosphorylation (Supplementary Fig. S2B). Collectively, these results demonstrate that neurofibromin regulation of astrocyte proliferation is mediated by PI3K/Akt activation.

PI3K Inhibition Decreases Optic Nerve Volume and Glioma Proliferation In vivo

Based on the observation that neurofibromin regulation of astrocyte proliferation is dependent on Akt activation, we next determined whether PI3K/Akt inhibition would effectively inhibit *Nf1* murine optic glioma growth. We initially evaluated MK2206, an allosteric Akt inhibitor[28]; however, this compound did not efficiently cross the blood–brain barrier (data not shown).

Since published reports employed BKM120, a PI3K inhibitor, to treat rodent intracranial glioblastoma,[29] we focused on this compound for our preclinical experiments. Following dose tolerability studies using 20, 40, and 60 mg/kg BKM120 administration by oral gavage (5 d/wk × 4 wk), we found that 20 mg/kg BKM120 was well tolerated. FMC mice were randomly assigned to receive either vehicle or 20 mg/kg BKM120 for 4 weeks ($n = 7–9$ mice/group). At the end of treatment, Akt phosphorylation (Thr308 and Ser473) and mTOR activation (S6-Ser240/244 phosphorylation) were inhibited in BKM120-treated mice relative to vehicle-treated controls (Fig. 3A), without any change in ERK phosphorylation (Supplementary Fig. S2C). Examination of optic nerves revealed that BKM120 treatment restored optic nerve volumes to wild-type levels and inhibited tumor proliferation (2.8-fold) (Fig. 3B) and mTOR activation (1.7-fold) compared with vehicle-treated FMC mice (Fig. 3C). Collectively, these observations establish that PI3K/Akt-mediated mTOR pathway activation underlies the increase in *Nf1*-deficient glial cell proliferation in vitro and in vivo.

MEK Inhibition Suppresses Neurofibromin-Dependent mTOR Activation and Astrocyte Proliferation In vitro

Recent studies have shown that MEK/ERK pathway activation is also critical for the growth of other NF1-associated tumor types.[14,15] To determine the contribution of MEK/ERK activation to the regulation of *Nf1*-deficient astrocyte proliferation, we employed a specific pharmacologic inhibitor of MEK, PD0325901 (PD901). Treatment of *Nf1*-deficient astrocytes with PD901 (1 nM) inhibited ERK phosphorylation (Fig. 4A) and reduced proliferation to wild-type levels (Fig. 4B). Based on previous observations that mTOR activation is central for neurofibromin regulation of astrocyte proliferation,[11,25] we next explored the possibility that ERK might regulate mTOR

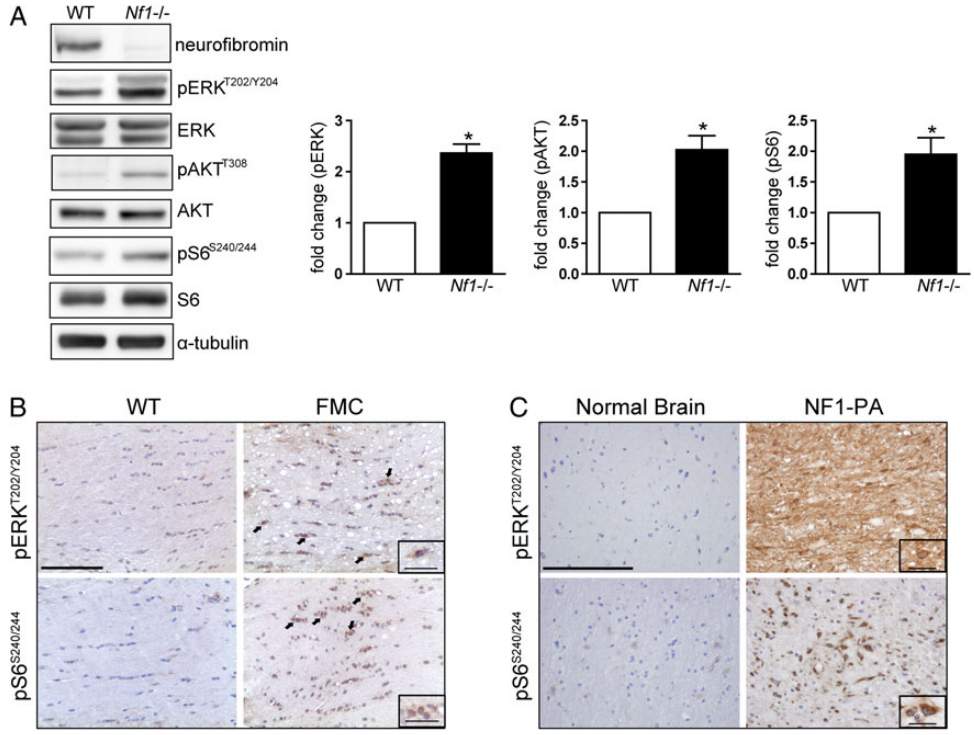

Fig. 1. Neurofibromin loss results in increased Ras effector activation. (A) *Nf1* loss results in increased ERK, Akt, and S6 phosphorylation ($pERK^{T202/Y204}$, $pAkt^{308}$, and $pS6^{S240/244}$, respectively) relative to wild-type (WT) controls following normalization to total ERK, Akt, and S6 levels (bar graphs). Representative Western blot of at least 4 independent replicate experiments. α-Tubulin was included as an internal loading control. Increased ERK and S6 phosphorylation was observed in (B) the optic nerves of FMC mice ($n = 9$) compared with age-matched $Nf1^{flox/flox}$ (WT) littermates ($n = 5$) (scale bar, 100 μm) and (C) human NF1-associated pilocytic astrocytomas (NF1-PA) ($n = 4$) relative to normal brain ($n = 4$) (scale bar, 200 μm). Arrows and insets denote representative immunopositive cells. Inset scale bar, 25 μm. $^*P < .05$. Bar graph denotes mean ± SEM.

activity.[30,31] While MEK inhibition had no effect on Akt activity in *Nf1*-deficient astrocytes in vitro (Fig. 4C) or in vivo (Supplementary Fig. S3A), PD901 treatment restored mTOR hyperactivation (increased $S6^{Ser\ 240/244}$ phosphorylation) to wild-type levels (Fig. 4A), indicating that MEK regulates mTOR activation in *Nf1*-deficient astrocytes.

Two established intermediates through which MEK/ERK can activate mTOR include the tuberous sclerosis complex (TSC)[32] and p90-ribosomal S6 kinase (p90RSK).[31] Since previous studies from our laboratory have demonstrated that neurofibromin regulation of mTOR activation in astrocytes does not require TSC/Rheb function,[25] we focused on p90RSK. In *Nf1*-deficient astrocytes, there was increased p90RSK phosphorylation (Thr573; 15-fold) relative to wild-type astrocytes (Supplementary Fig. S3B). Consistent with ERK regulation of p90RSK activity, the observed increase in p90RSK phosphorylation was inhibited following PD901 treatment (Supplementary Fig. S3B). Furthermore, treatment with a specific p90RSK inhibitor (SL0101; 100 μM) reduced S6 phosphorylation (Ser235/236 and Ser240/244, 2.6- and 4.2-fold, respectively) (Supplementary Fig. S3C) and proliferation (Supplementary Fig. S3D) in *Nf1*-deficient astrocytes. While p90RSK has also been shown to phosphorylate S6 on serine residues 235 and 236 in an mTOR-independent manner,[30] the observation that both PD901 and SL0101 inhibit the S6 phosphorylation on serine residues 240 and 244, established mTOR/p70S6K-specific phosphorylation sites,[30] suggests that MEK/ERK/RSK regulation of *Nf1*-deficient astrocyte proliferation operates at the level of mTOR. Collectively, these results demonstrate that MEK/ERK activation increases *Nf1*-deficient astrocyte growth by activating mTOR.

MEK Inhibition Decreases Optic Nerve Volume and Glioma Proliferation In vivo

Based on the observation that neurofibromin regulation of astrocyte proliferation is also dependent on MEK activation of mTOR, we next determined whether MEK inhibition would reduce *Nf1* murine optic glioma growth in vivo. In these preclinical studies, FMC mice were randomized in 2 groups ($n = 7–10$ mice/group). Group 1 received the MEK inhibitor (5 mg/kg PD901) once daily by oral gavage for 4 weeks, while group 2 was given vehicle alone. Using this dosing regimen, PD901 treatment did not reduce optic nerve volume or glioma proliferation (data not shown).

Next, to exclude the possibility that this lack of efficacy reflected inadequate target inhibition in the brain, we performed additional pharmacodynamic studies. In these experiments, we assessed the duration of target inhibition in the brain following PD901 treatment. Mice received 5 mg/kg PD901 for 5 days, and target inhibition was measured at 0, 2, and 12 h ($n = 3$ mice per time point). While there was ERK inhibition

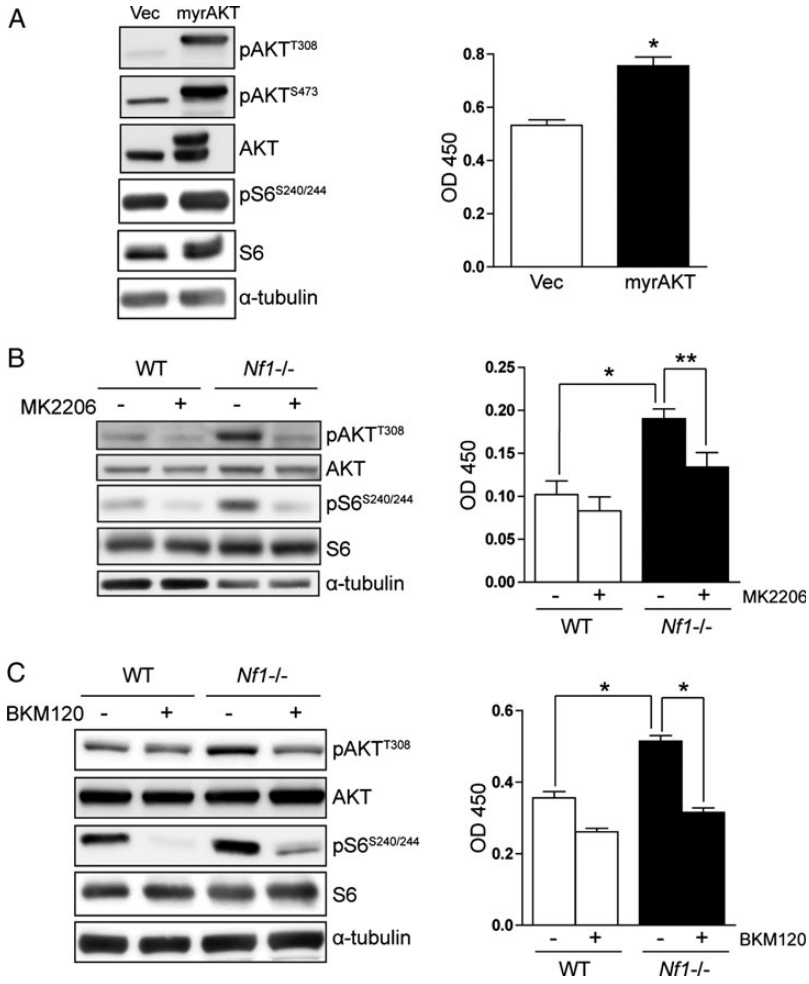

Fig. 2. Neurofibromin regulates astrocyte proliferation in a PI3K/Akt-dependent manner in vitro. (A) Ectopic expression of a constitutively active Akt (myrAkt) molecule results in increased astrocyte proliferation (right). Western blot demonstrates increased Akt activation (Thr^{308} and Ser^{473} phosphorylation) and mTOR activation (pS6$^{Ser240/244}$ phosphorylation) following myrAkt expression. (B) Treatment with the MK2206 Akt inhibitor (50 nM) or (C) the BKM120 PI3K inhibitor (5 nM) reduces the increased Akt activation, S6 activation, and proliferation observed in *Nf1*−/− astrocytes to wild-type (WT) levels. *$P < .01$, **$P < .05$. Bar graph denotes mean ± SEM. The data are representative of 3 independent replicate experiments.

(pERK) at 2 h, ERK was no longer inhibited at the 12 h time point (Fig. 5A). These data suggest that the lack of efficacy observed in the original preclinical trial likely reflected suboptimal target inhibition in the brain.

Based on previous reports that prolonged inhibition of ERK activity is necessary for therapeutic efficacy,[14,33] we next assessed twice-a-day PD901 dosing in *Nf1* optic glioma mice. For this study, mice received either vehicle or 5 mg/kg PD901 twice daily for 4 weeks. Using this dosing schedule, MEK inhibition decreased optic glioma volumes and proliferation (Fig. 5B) to wild-type levels. Moreover, target inhibition (reduced ERK phosphorylation) was observed in the optic nerves of FMC mice following PD901 treatment, and, similar to our observations in vitro, there was a concomitant inhibition of S6 phosphorylation in the optic nerves of PD901-treated mice (Fig. 5C). Taken together, these results indicate that MEK/ERK inhibition reduces murine *Nf1* optic glioma growth by attenuating mTOR activation.

PI3K or MEK Inhibition Improves Retinal Dysfunction in FMC Mice

Thirty percent to 50% of children with NF1-OPG experience reduced visual acuity,[4,5] and many of those who underwent chemotherapy did not show improved vision following treatment.[5,34] To assess the impact of PD901 and BKM120 treatment on optic glioma–induced retinal dysfunction, we analyzed RGC survival and RNFL thickness. We previously demonstrated that FMC mice exhibit RGC death and thinning of RNFL associated with reduced visual acuity.[20,35] However, following treatment, we observed 1.9-fold and 4.9-fold decreases in TUNEL$^+$ cells in BKM120-treated (Fig. 6A) and PD901-treated (Fig. 6B) mice, respectively, relative to vehicle-treated controls. Similarly, BKM120-treated (Fig. 6A) and PD901-treated (Fig. 6B) mice retained averages of 40% (range, 14%–57%) and 50% (range, 34%–60%), respectively, more RGCs (%Brn3a$^+$ cells) than vehicle-treated controls. Lastly, RNFL thickness following

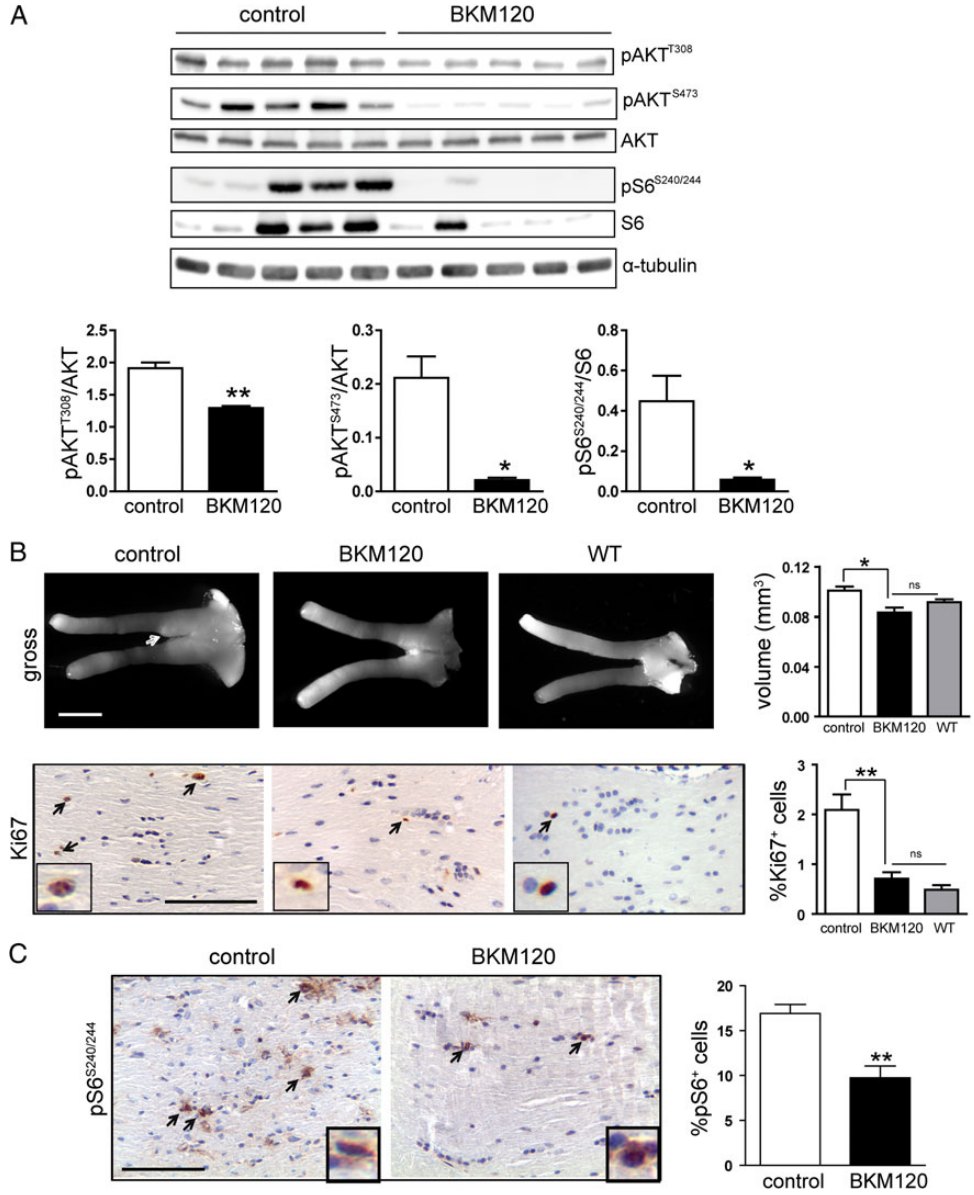

Fig. 3. PI3K inhibition decreases optic nerve volume and glioma proliferation. (A) Western blot from representative animals demonstrates Akt and mTOR target inhibition in the brains of FMC mice treated with 20 mg/kg BKM120. Bar graphs in the lower panel show the quantification of $pAkt^{T308}$, $pAkt^{S473}$, and $pS6^{S240/244}$ relative to the respective total proteins. α-Tubulin was included as an internal protein loading control. (B) The optic nerves of BKM120-treated mice ($n = 9$) have reduced volumes (scale bar, 1000 μm, arrow, tumor region) and proliferation (%$Ki67^+$ cells) similar to that observed in $Nf1^{flox/flox}$ (wild-type [WT], $n = 6$) mice. (C) Treatment of mice with BKM120 inhibits optic nerve S6 activation (%$pS6^+$ cells; scale bar 100 μm) compared with vehicle-treated mice ($n = 7$). $^*P < .01$, $^{**}P < .001$. Bar graph denotes mean ± SEM. Arrows and insets denote representative immunopositive cells. ns, not significant.

BKM120 (Fig. 6A) and PD901 (Fig. 6B) treatment was increased by 1.6-fold and 2.3-fold, respectively, relative to vehicle-treated FMC mice. These data demonstrate that PI3K and MEK inhibitors improve retinal pathology in the setting of murine *Nf1* optic glioma.

Discussion

NF1 is a disorder of heterogeneity, which operates at the genomic, tissue, cellular, and molecular levels. This heterogeneity complicates the design of effective clinical trials, as results obtained using one tissue type may not be translatable to a different cell type. In this regard, previous studies have revealed that neurofibromin regulates osteoclast function in either a MEK/Rho-, Rac1-, or Akt/mTOR-dependent manner,[36–38] whereas *Nf1*+/− osteoblasts and microglia are dependent on c-Jun NH(2)-terminal kinase signaling.[39,40] In contrast, MEK activation underlies the growth of *Nf1* murine leukemic cells.[14] Furthermore, while *Nf1*-deficient peripheral nervous system neuron function is dependent on PI3K/Akt signaling,[41]

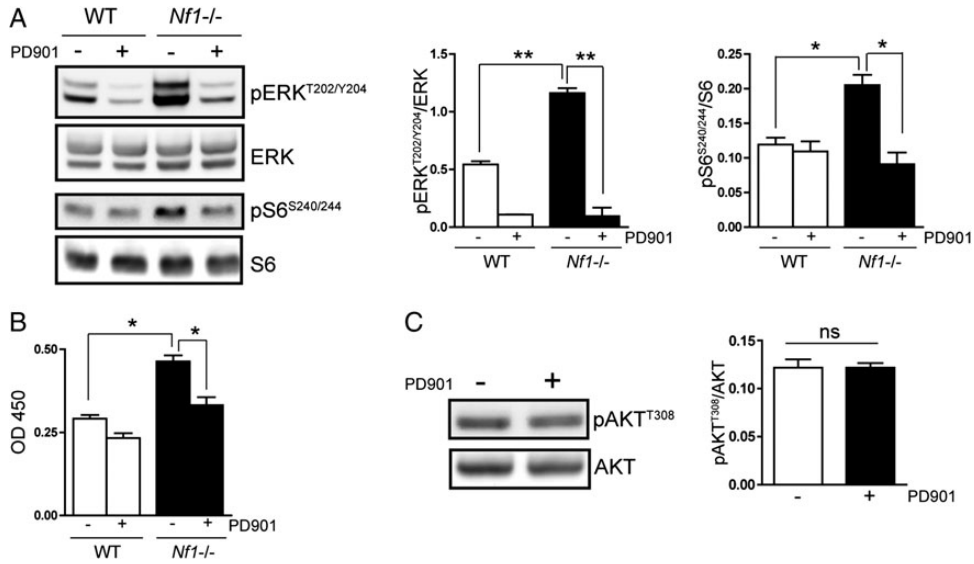

Fig. 4. MEK inhibition suppresses *Nf1*-deficient astrocyte proliferation in an mTOR-dependent manner in vitro. (A) Treatment with the MEK inhibitor PD901 (1 nM) restores the ERK and S6 hyperphosphorylation observed in *Nf1*-deficient astrocytes to wild-type (WT) levels. Bar graphs show the quantification of $pERK^{T202/Y204}$ and $pS6^{S240/244}$ relative to their respective total proteins. (B) PD901 treatment reduces *Nf1*-deficient astrocyte proliferation to WT levels. (C) MEK inhibition (PD901) does not reduce Akt activation (T308) in *Nf1*-deficient astrocytes in vitro. $^{*}P < .01$, $^{**}P < .001$; ns, not significant. Bar graph denotes mean ± SEM. Data are representative of 3 independent replicate experiments.

Nf1+/− central nervous system neurons do not rely on Akt signaling, but rather are dependent on cyclic AMP homeostasis.[42]

In the current report, we leveraged *Nf1* GEMs to define the targetable Ras downstream signaling pathways critical for regulating *Nf1*-deficient astrocyte and *Nf1* optic glioma growth. In both *Nf1*-deficient astrocytes and *Nf1* optic gliomas, there was increased Akt, ERK, and mTOR activation. Following PI3K/Akt inhibition, we observed reduced *Nf1*-deficient astrocyte proliferation in vitro and *Nf1* optic glioma proliferation in vivo. In addition, in response to sustained pharmacologic MEK blockade, there was attenuated *Nf1*-deficient astrocyte and *Nf1* optic glioma proliferation. This latter inhibition of *Nf1*-deficient astrocyte and *Nf1* optic glioma growth reflects the ability of ERK to activate mTOR without affecting Akt activity. Collectively, these findings establish MEK/ERK- and PI3K/Akt-dependent mTOR activation as critical drivers of NF1-associated glioma maintenance.

Previous studies using murine malignant peripheral nerve sheath tumor (MPNST) model systems have demonstrated that either MEK[15,43] or mTOR[44,45] inhibition reduces MPNST growth in vivo. These findings suggest that these tumors might be reliant on 2 distinct, non-interacting pathways. An alternative explanation, as revealed by the current study, is that MEK/ERK and PI3K/Akt signaling downstream of Ras in *Nf1*-deficient tumor cells converge on a single effector pathway (mTOR) to regulate cell growth. As such, effective pharmacologic silencing of mTOR might suffice for optimal efficacy.

However, it is also possible that neurofibromin-Ras regulation of cell growth reflects the independent consequences of each downstream effector arm. For example, in *Nf1*−/− leukemic cells, MEK/ERK signaling controls proliferation, while PI3K/Akt signaling is responsible for survival.[46] Similarly, in *Nf1*+/− mast cells, Pak1/MEK activation leads to increased proliferation, whereas Pak1/p38–mitogen-activated protein kinase activity accounts for the increased migration of these cells.[47] However, in *Nf1* murine optic glioma, we observed no change in apoptosis in vivo (Supplementary Fig. S4A). In addition, *Nf1*-deficient astrocytes exhibited no change in autophagy relative to their wild-type counterparts (Supplementary Fig. S4B), suggesting that different biological functions do not account for the differences in MEK/ERK- versus PI3K/Akt-mediated mTOR regulation.

It is equally possible that the Ras downstream effector pathways exhibit some level of cross-talk and, in this manner, influence each other's function. Precedent for this derives from studies on *Nf1*+/− mast cells in which PI3K activation increases MEK activity.[48] However, in *Nf1*-deficient astrocytes and *Nf1* optic gliomas in vitro and in vivo, MEK inhibition had no effect on Akt activity and PI3K/Akt inhibition did not reduce ERK activity. These findings argue against cross-talk as the explanation for the dependence of *Nf1*-deficient astrocytes and optic gliomas on mTOR signaling.

Instead, we favor the hypothesis that mTOR activation by either PI3K/Akt or MEK/ERK in *Nf1*-deficient glial cells in vitro and in vivo reflects distinct mechanisms of mTOR regulation. Previous studies in our laboratory using different neuroglial cell types and glioma-associated mutations have revealed divergent ways by which mTOR can be regulated. For example, expression of *KIAA1549:BRAF*, the signature pediatric low-grade glioma genetic rearrangement, activates MEK signaling in neural stem cells and leads to increased mTOR activation through ERK-dependent TSC-2 protein (tuberin) phosphorylation.[49] However, Akt-dependent mTOR activation in *Nf1*-deficient astrocytes occurs in a TSC/Rheb-independent manner.[25] In these studies, neurofibromin loss in astrocytes had no effect on tuberin phosphorylation, and small hairpin RNA–mediated silencing of Rheb expression did not reduce the mTOR

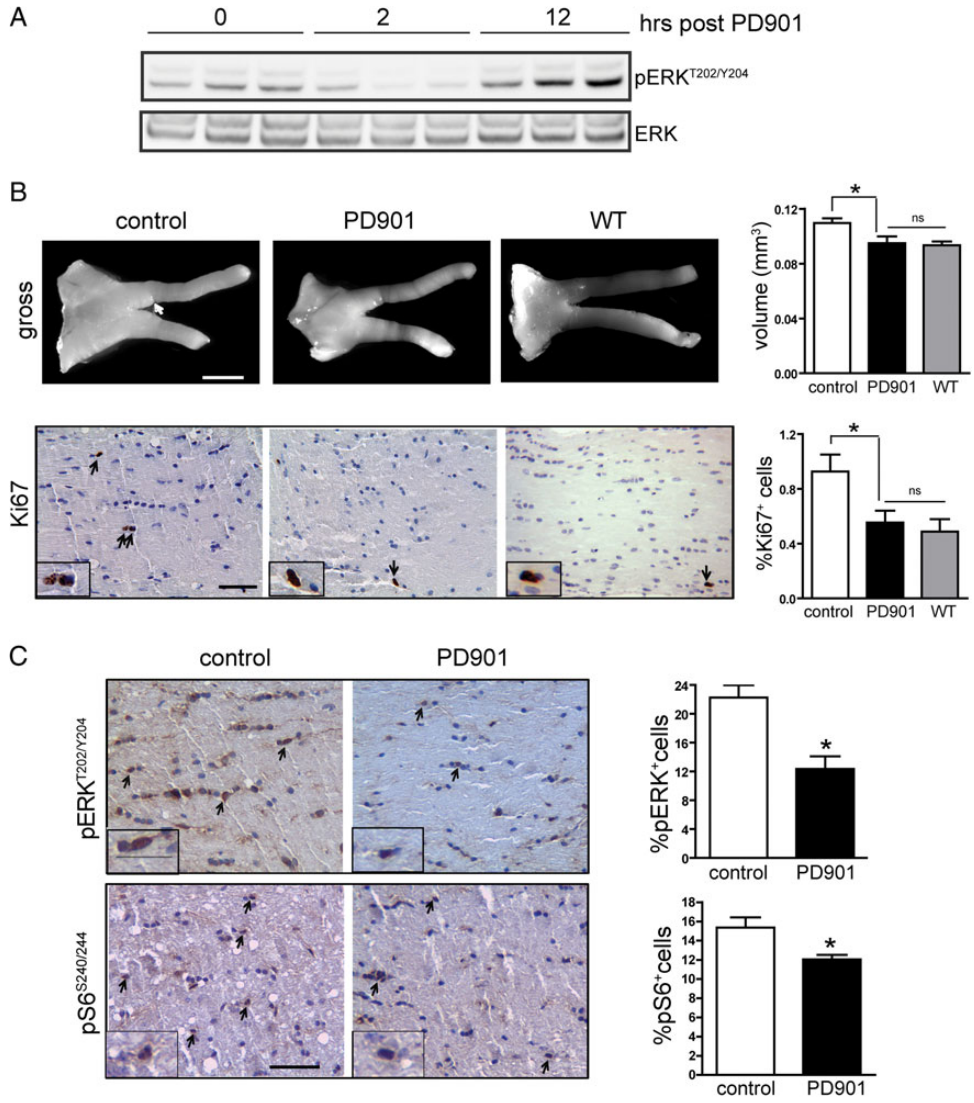

Fig. 5. Sustained MEK inhibition decreases *Nf1* mouse optic glioma volume and proliferation. (A) Western blot demonstrates ERK$^{T202/Y204}$ phosphorylation at 0, 2, and 12 h following a 5-day treatment of PD901 (5 mg/kg, once a day; $n = 3$ mice per time point). (B) FMC mice treated with 5 mg/kg PD901 twice daily ($n = 8$) for 4 weeks have reduced optic glioma tumor volumes (scale bar, 1000 μm, arrow, tumor region) and proliferation (%Ki67$^+$ cells), comparable to *Nf1*$^{flox/flox}$ (wild-type [WT], $n = 6$) mice. (C) PD901-treated mice have reduced ERK activation (%pERK$^+$ cells) and S6 activation (%pS6$^+$ cells) compared with vehicle-treated mice ($n = 6$). Scale bar, 50 μm. Arrows and insets denote representative immunopositive cells. *$P < .05$. Bar graph denotes mean ± SEM; ns, not significant.

hyperactivation or increased proliferation observed in *Nf1*-deficient astrocytes.

To determine how MEK/ERK hyperactivation leads to increased mTOR signaling in *Nf1*-deficient astrocytes, we examined p90RSK phosphorylation. Previous studies in other cell types have shown that p90RSK phosphorylates S6 either directly (exclusively on Ser$^{235/236}$) or indirectly via Raptor phosphorylation and downstream mTOR complex 1 signaling.[30,31] We demonstrate that p90RSK activation in *Nf1*-deficient astrocytes is regulated by MEK, such that the increase in S6 activity and proliferation is reduced to wild-type levels following pharmacologic p90RSK inhibition. It is worth noting that MEK inhibition reduces S6 (Ser$^{240/244}$) phosphorylation in *Nf1*-deficient astrocytes, consistent with p90RSK regulation of mTOR activity, perhaps at the level of Raptor/mTOR complex 1 function. The finding that p90RSK inhibition likewise reduces S6 (Ser$^{240/244}$) phosphorylation as well as proliferation in *Nf1*-deficient astrocytes further supports this mode of MEK-dependent mTOR regulation. Additional studies will be required to elucidate the precise mechanism by which ERK and p90RSK regulate mTOR activation in *Nf1*-deficient astrocytes.

Finally, most children with NF1-OPG are treated for declining visual acuity.[4,5] To determine the effect of pharmacologic treatments on this clinically important consequence of brain tumor burden in the setting of NF1, we assessed retinal dysfunction in mice treated with BKM120 or PD901. In contrast to some genotoxic drugs, like temozolomide, which actually increase RGC apoptosis (J.A.T., unpublished observations) while decreasing

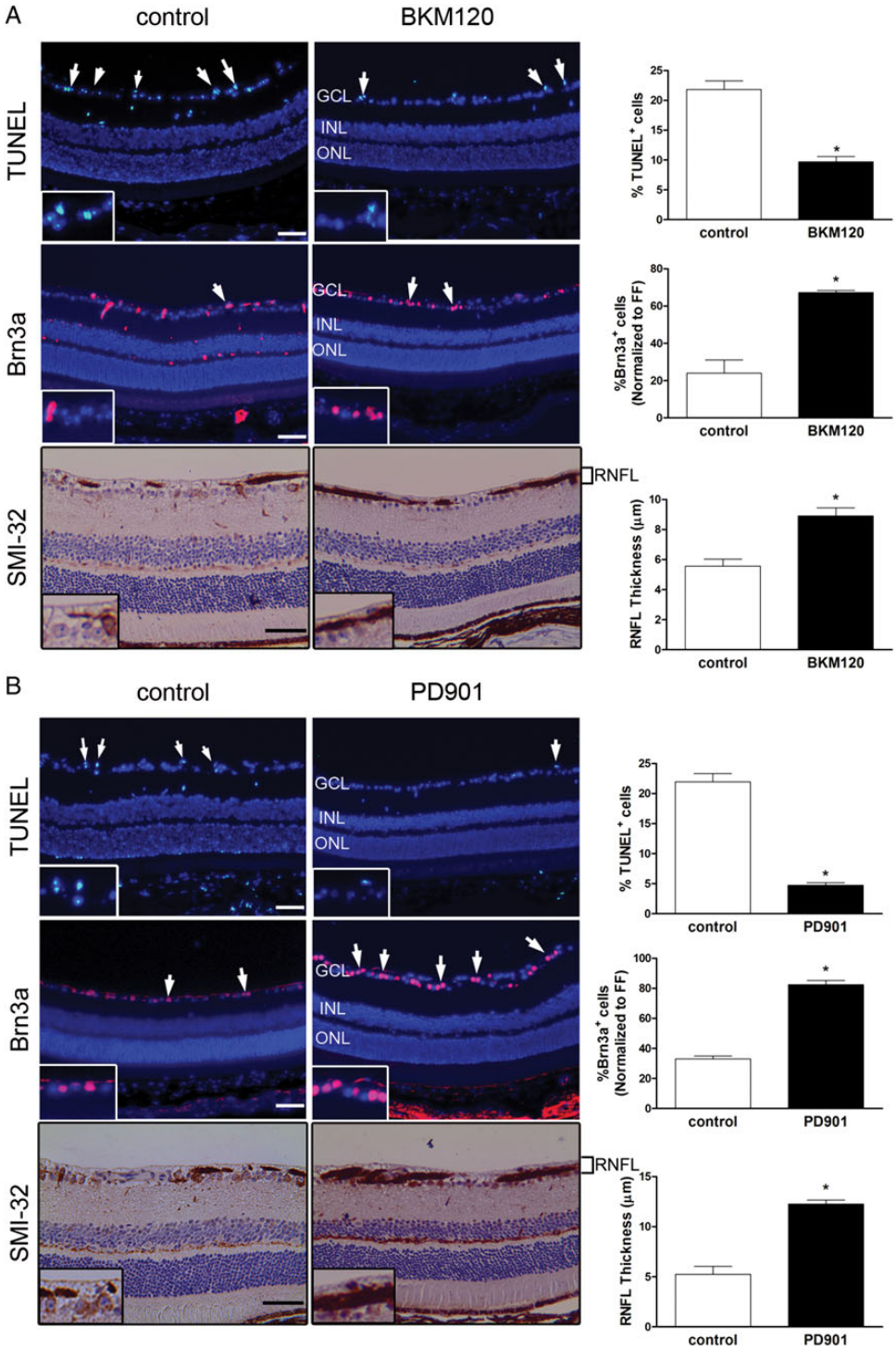

Fig. 6. PI3K and MEK inhibition attenuates retinal dysfunction in FMC mice in vivo. (A) TUNEL staining ($n = 4$; top panels), Brn3a immunofluorescence ($n = 5$; middle panels), and SMI-32 immunohistochemistry ($n = 4$; bottom panels) demonstrate a decrease in apoptosis, restored Brn3a cell numbers (normalized to wild-type [FF] mice), and increased RNFL thickness, respectively, following BKM120 treatment relative to vehicle-treated controls. (B) TUNEL staining ($n = 4$; top panels), Brn3a immunofluorescence ($n = 5$; middle panels), and SMI-32 immunohistochemistry ($n = 4$; bottom panels) demonstrate a decrease in apoptosis, restored Brn3a cell numbers (normalized to wild-type [FF] mice), and increased RNFL thickness, respectively, following PD901 treatment relative to vehicle-treated controls. Individual $TUNEL^+$ and $Brn3a^+$ cells within the ganglion cell layer (GCL) and $SMI\text{-}32^+$ RNFL axons are shown in the insets. Quantification is represented in the adjacent graphs. INL, inner nuclear layer; ONL, outer nuclear layer. $^*P < .05$. Bar graph denotes mean ± SEM. Arrows and insets denote representative immunopositive cells. Scale bar, 50 μm.

mouse optic glioma volume and proliferation,[13] both of these biologically targeted agents attenuated RGC apoptosis and RNFL thinning. Current studies are in progress to evaluate the efficacy of these treatments on RGC layer integrity using ocular coherence tomography[50] and visual function[35] in *Nf1* GEM strains.

In summary, this report raises important issues relevant to the deployment of preclinical mouse modeling to inform future clinical trials. First, 2 independent arms of the Ras effector pathway (MEK/ERK, PI3K/Akt) can individually influence *Nf1* optic glioma growth. Second, these 2 pathways converge on mTOR as a central regulator of *Nf1* optic glioma maintenance using distinct mechanisms. Third, future studies should be focused on optimizing mTOR inhibition using either combination therapies or single-agent approaches. In this regard, it is possible that the combined use of agents targeting mTOR through different effector arms and signaling intermediates may synergize to result in tumor cell apoptosis and more durable effects on NF1-OPG outcome. The use of GEMs and pharmacologic inhibitors strengthens the case for the use of biologically based therapies that target mTOR deregulation for the treatment of NF1-associated brain tumors.

Supplementary Material

Supplementary material is available online at *Neuro-Oncology* (http://neuro-oncology.oxfordjournals.org/).

Funding

This work was supported by a grant from the National Cancer Institute (U01CA141549 to D.H.G.).

Acknowledgments

We thank Ryan Emnett for technical assistance, Dr Sonika Dahiya (Neuropathology, Washington University School of Medicine) for expert advice, and Novartis for providing the NVP-BKM120 compound. We appreciate the advice of members of the Children's Tumor Foundation Preclinical Consortium during the initial phases of this project.

Conflict of interest statement. The authors declare no conflicts of interest.

References

1. Gutmann DH, Aylsworth A, Carey JC, et al. The diagnostic evaluation and multidisciplinary management of neurofibromatosis 1 and neurofibromatosis 2. *JAMA*. 1997;278(1):51–57.
2. Listernick R, Charrow J, Greenwald M, et al. Natural history of optic pathway tumors in children with neurofibromatosis type 1: a longitudinal study. *J Pediatr*. 1994;125(1):63–66.
3. Listernick R, Charrow J, Greenwald MJ, et al. Optic gliomas in children with neurofibromatosis type 1. *J Pediatr*. 1989;114(5):788–792.
4. Listernick R, Ferner RE, Liu GT, et al. Optic pathway gliomas in neurofibromatosis-1: controversies and recommendations. *Ann Neurol*. 2007;61(3):189–198.
5. Fisher MJ, Loguidice M, Gutmann DH, et al. Visual outcomes in children with neurofibromatosis type 1–associated optic pathway glioma following chemotherapy: a multicenter retrospective analysis. *Neuro Oncol*. 2012;14(6):790–797.
6. Sharif S, Ferner R, Birch JM, et al. Second primary tumors in neurofibromatosis 1 patients treated for optic glioma: substantial risks after radiotherapy. *J Clin Oncol*. 2006;24(16):2570–2575.
7. Mahoney DH Jr., Cohen ME, Friedman HS, et al. Carboplatin is effective therapy for young children with progressive optic pathway tumors: a Pediatric Oncology Group phase II study. *Neuro Oncol*. 2000;2(4):213–220.
8. Packer RJ, Lange B, Ater J, et al. Carboplatin and vincristine for recurrent and newly diagnosed low-grade gliomas of childhood. *J Clin Oncol*. 1993;11(5):850–856.
9. Bajenaru ML, Garbow JR, Perry A, et al. Natural history of neurofibromatosis 1–associated optic nerve glioma in mice. *Ann Neurol*. 2005;57(1):119–127.
10. Bajenaru ML, Hernandez MR, Perry A, et al. Optic nerve glioma in mice requires astrocyte Nf1 gene inactivation and Nf1 brain heterozygosity. *Cancer Res*. 2003;63(24):8573–8577.
11. Dasgupta B, Yi Y, Chen DY, et al. Proteomic analysis reveals hyperactivation of the mammalian target of rapamycin pathway in neurofibromatosis 1-associated human and mouse brain tumors. *Cancer Res*. 2005;65(7):2755–2760.
12. Dasgupta B, Li W, Perry A, et al. Glioma formation in neurofibromatosis 1 reflects preferential activation of K-RAS in astrocytes. *Cancer Res*. 2005;65(1):236–245.
13. Hegedus B, Banerjee D, Yeh TH, et al. Preclinical cancer therapy in a mouse model of neurofibromatosis-1 optic glioma. *Cancer Res*. 2008;68(5):1520–1528.
14. Chang T, Krisman K, Theobald EH, et al. Sustained MEK inhibition abrogates myeloproliferative disease in Nf1 mutant mice. *J Clin Invest*. 2013;123(1):335–339.
15. Jessen WJ, Miller SJ, Jousma E, et al. MEK inhibition exhibits efficacy in human and mouse neurofibromatosis tumors. *J Clin Invest*. 2013;123(1):340–347.
16. Maira SM, Pecchi S, Huang A, et al. Identification and characterization of NVP-BKM120, an orally available pan-class I PI3-kinase inhibitor. *Mol Cancer Ther*. 2012;11(2):317–328.
17. Yeh TH, Lee da Y, Gianino SM, et al. Microarray analyses reveal regional astrocyte heterogeneity with implications for neurofibromatosis type 1 (NF1)–regulated glial proliferation. *Glia*. 2009;57(11):1239–1249.
18. Uhlmann EJ, Li W, Scheidenhelm DK, et al. Loss of tuberous sclerosis complex 1 (Tsc1) expression results in increased Rheb/S6 K pathway signaling important for astrocyte cell size regulation. *Glia*. 2004;47(2):180–188.
19. Hegedus B, Yeh TH, Lee da Y, et al. Neurofibromin regulates somatic growth through the hypothalamic-pituitary axis. *Hum Mol Genet*. 2008;17(19):2956–2966.
20. Kaul A, Toonen JA, Gianino SM, et al. The impact of coexisting genetic mutations on murine optic glioma biology. *Neuro Oncol*. 2014(1–8): doi:10.1093/neuonc/nou287.
21. Bollag G, Clapp DW, Shih S, et al. Loss of NF1 results in activation of the Ras signaling pathway and leads to aberrant growth in haematopoietic cells. *Nat Genet*. 1996;12(2):144–148.
22. DeClue JE, Papageorge AG, Fletcher JA, et al. Abnormal regulation of mammalian p21ras contributes to malignant tumor growth in von Recklinghausen (type 1) neurofibromatosis. *Cell*. 1992;69(2):265–273.

23. Solga AC, Gianino SM, Gutmann DH. NG2-cells are not the cell of origin for murine neurofibromatosis-1 (Nf1) optic glioma. *Oncogene*. 2014;33(3):289–299.
24. Guillamo JS, Creange A, Kalifa C, et al. Prognostic factors of CNS tumours in neurofibromatosis 1 (NF1): a retrospective study of 104 patients. *Brain*. 2003;126:(Pt 1):152–160.
25. Banerjee S, Crouse NR, Emnett RJ, et al. Neurofibromatosis-1 regulates mTOR-mediated astrocyte growth and glioma formation in a TSC/Rheb-independent manner. *Proc Natl Acad Sci U S A*. 2011;108(38):15996–16001.
26. Johannessen CM, Reczek EE, James MF, et al. The NF1 tumor suppressor critically regulates TSC2 and mTOR. *Proc Natl Acad Sci U S A*. 2005;102(24):8573–8578.
27. Boehm JS, Zhao JJ, Yao J, et al. Integrative genomic approaches identify IKBKE as a breast cancer oncogene. *Cell*. 2007;129(6):1065–1079.
28. Hirai H, Sootome H, Nakatsuru Y, et al. MK-2206, an allosteric Akt inhibitor, enhances antitumor efficacy by standard chemotherapeutic agents or molecular targeted drugs in vitro and in vivo. *Mol Cancer Ther*. 2010;9(7):1956–1967.
29. Koul D, Fu J, Shen R, et al. Antitumor activity of NVP-BKM120--a selective pan class I PI3 kinase inhibitor showed differential forms of cell death based on p53 status of glioma cells. *Clin Cancer Res*. 2012;18(1):184–195.
30. Roux PP, Shahbazian D, Vu H, et al. RAS/ERK signaling promotes site-specific ribosomal protein S6 phosphorylation via RSK and stimulates cap-dependent translation. *J Biol Chem*. 2007;282(19):14056–14064.
31. Carriere A, Cargnello M, Julien LA, et al. Oncogenic MAPK signaling stimulates mTORC1 activity by promoting RSK-mediated raptor phosphorylation. *Curr Biol*. 2008;18(17):1269–1277.
32. Ma L, Chen Z, Erdjument-Bromage H, et al. Phosphorylation and functional inactivation of TSC2 by Erk implications for tuberous sclerosis and cancer pathogenesis. *Cell*. 2005;121(2):179–193.
33. Lauchle JO, Kim D, Le DT, et al. Response and resistance to MEK inhibition in leukaemias initiated by hyperactive Ras. *Nature*. 2009;461(7262):411–414.
34. Kalin-Hajdu E, Decarie JC, Marzouki M, et al. Visual acuity of children treated with chemotherapy for optic pathway gliomas. *Pediatr Blood Cancer*. 2014;61(2):223–227.
35. Diggs-Andrews KA, Brown JA, Gianino SM, et al. Sex is a major determinant of neuronal dysfunction in neurofibromatosis type 1. *Ann Neurol*. 2014;75(2):309–316.
36. Yan J, Chen S, Zhang Y, et al. Rac1 mediates the osteoclast gains-in-function induced by haploinsufficiency of Nf1. *Hum Mol Genet*. 2008;17(7):936–948.
37. Stevenson DA, Yan J, He Y, et al. Multiple increased osteoclast functions in individuals with neurofibromatosis type 1. *Am J Med Genet A*. 2011;155A(5):1050–1059.
38. Ma J, Li M, Hock J, et al. Hyperactivation of mTOR critically regulates abnormal osteoclastogenesis in neurofibromatosis type 1. *J Orthop Res*. 2012;30(1):144–152.
39. Sullivan K, El-Hoss J, Little DG, et al. JNK inhibitors increase osteogenesis in Nf1-deficient cells. *Bone*. 2011;49(6):1311–1316.
40. Daginakatte GC, Gianino SM, Zhao NW, et al. Increased c-Jun-NH2-kinase signaling in neurofibromatosis-1 heterozygous microglia drives microglia activation and promotes optic glioma proliferation. *Cancer Res*. 2008;68(24):10358–10366.
41. Klesse LJ, Parada LF. p21 ras and phosphatidylinositol-3 kinase are required for survival of wild-type and NF1 mutant sensory neurons. *J Neurosci*. 1998;18(24):10420–10428.
42. Brown JA, Gianino SM, Gutmann DH. Defective cAMP generation underlies the sensitivity of CNS neurons to neurofibromatosis-1 heterozygosity. *J Neurosci*. 2010;30(16):5579–5589.
43. Dodd RD, Mito JK, Eward WC, et al. NF1 deletion generates multiple subtypes of soft-tissue sarcoma that respond to MEK inhibition. *Mol Cancer Ther*. 2013;12(9):1906–1917.
44. Johansson G, Mahller YY, Collins MH, et al. Effective in vivo targeting of the mammalian target of rapamycin pathway in malignant peripheral nerve sheath tumors. *Mol Cancer Ther*. 2008;7(5):1237–1245.
45. Johannessen CM, Johnson BW, Williams SM, et al. TORC1 is essential for NF1-associated malignancies. *Curr Biol*. 2008;18(1):56–62.
46. Donovan S, See W, Bonifas J, et al. Hyperactivation of protein kinase B and ERK have discrete effects on survival, proliferation, and cytokine expression in Nf1-deficient myeloid cells. *Cancer Cell*. 2002;2(6):507–514.
47. McDaniel AS, Allen JD, Park SJ, et al. Pak1 regulates multiple c-Kit mediated Ras-MAPK gain-in-function phenotypes in Nf1+/− mast cells. *Blood*. 2008;112(12):4646–4654.
48. Ingram DA, Hiatt K, King AJ, et al. Hyperactivation of p21(ras) and the hematopoietic-specific Rho GTPase, Rac2, cooperate to alter the proliferation of neurofibromin-deficient mast cells in vivo and in vitro. *J Exp Med*. 2001;194(1):57–69.
49. Kaul A, Chen YH, Emnett RJ, et al. Pediatric glioma-associated KIAA1549:BRAF expression regulates neuroglial cell growth in a cell type-specific and mTOR-dependent manner. *Genes Dev*. 2012;26(23):2561–2566.
50. Avery RA, Hwang EI, Ishikawa H, et al. Handheld optical coherence tomography during sedation in young children with optic pathway gliomas. *JAMA Ophthalmol*. 2014;132(3):265–271.